university of groningen

University Medical Center Groningen

University of Groningen

Enzymatic Biodiesel Synthesis by the Biphasic Esterification of Oleic Acid and 1-Butanol in Microreactors

Hommes, Arne; de Wit, Tom; Euverink, Gert-Jan; Yue, Jun

Published in:
Industrial & Engineering Chemistry Research

DOI:
10.1021/acs.iecr.9b02693

IMPORTANT NOTE: You are advised to consult the publisher's version (publisher's PDF) if you wish to cite from it. Please check the document version below.

Document Version
Publisher's PDF, also known as Version of record

Publication date:
2019

Link to publication in University of Groningen/UMCG research database

Citation for published version (APA):
Hommes, A., de Wit, T., Euverink, G-J., & Yue, J. (2019). Enzymatic Biodiesel Synthesis by the Biphasic Esterification of Oleic Acid and 1-Butanol in Microreactors. *Industrial & Engineering Chemistry Research*, *58*(34), 15432-15444. https://doi.org/10.1021/acs.iecr.9b02693

Copyright
Other than for strictly personal use, it is not permitted to download or to forward/distribute the text or part of it without the consent of the author(s) and/or copyright holder(s), unless the work is under an open content license (like Creative Commons).

The publication may also be distributed here under the terms of Article 25fa of the Dutch Copyright Act, indicated by the “Taverne” license. More information can be found on the University of Groningen website: https://www.rug.nl/library/open-access/self-archiving-pure/taverne-amendment.

Take-down policy
If you believe that this document breaches copyright please contact us providing details, and we will remove access to the work immediately and investigate your claim.

Downloaded from the University of Groningen/UMCG research database (Pure): http://www.rug.nl/research/portal. For technical reasons the number of authors shown on this cover page is limited to 10 maximum.

This is an open access article published under a Creative Commons Non-Commercial No Derivative Works (CC-BY-NC-ND) Attribution License, which permits copying and redistribution of the article, and creation of adaptations, all for non-commercial purposes.

I&EC research
Industrial & Engineering Chemistry Research

Article

Cite This: Ind. Eng. Chem. Res. 2019, 58, 15432−15444

pubs.acs.org/IECR

Enzymatic Biodiesel Synthesis by the Biphasic Esterification of Oleic Acid and 1-Butanol in Microreactors

Arne Hommes,[†] Tom de Wit,[†] Gerrit Jan Willem Euverink,[‡] and Jun Yue*[,†]

[†]Department of Chemical Engineering, Engineering and Technology Institute Groningen and [‡]Products and Processes for Biotechnology, University of Groningen, Nijenborgh 4, 9747 AG Groningen, The Netherlands

Supporting Information

ABSTRACT: The enzymatic esterification of oleic acid and 1-butanol to butyl oleate was performed in an aqueous−organic system in capillary microreactors with various inner diameters operated under slug flow. The free *Rhizomucor miehei* lipase in the aqueous phase was used as a catalyst and *n*-heptane as the organic solvent. A close to 100% yield of butyl oleate could be achieved in the microreactor made of polytetrafluoroethylene within 30 min residence time at 30 °C. The reaction rate is well described by the existing kinetic model based on a Ping Pong Bi Bi mechanism with competitive inhibition of 1-butanol. This model was extended to describe the effect of the interfacial area and aqueous-to-organic flow ratio in microreactors. By performing the reaction at low aqueous-to-organic flow ratios in hydrophilic microreactors (e.g., made of stainless steel), the enzyme turnover number could be enhanced significantly, making it promising for process intensification.

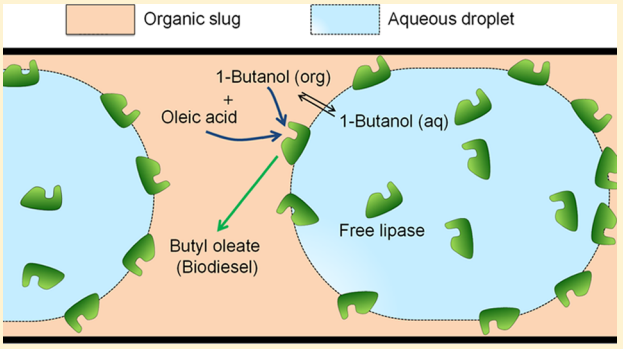

1. INTRODUCTION

Biodiesel is a promising renewable fuel that can be obtained from triglycerides and fatty acids present in bio-based oils (e.g., plant oils and waste cooking oils) and animal fats.[1−3] It is a potential and alternative transportation fuel to the conventional diesel derived from fossil resources. Besides its renewability, biodiesel has advantages that it is biodegradable and nontoxic, and its combustion results in lower sulfur, CO, and NO_x emissions than the conventional diesel.[4] The synthesis of biodiesel is typically realized by a transesterification reaction of triglycerides with a (bio-based) alcohol (e.g., methanol, ethanol, 1-butanol), where glycerol is formed as a side product. Besides triglycerides, bio-based oils may contain free fatty acids (e.g., oleic acid), water, and impurities.[2] Industrial biodiesel production is commonly performed using homogeneous alkali catalysts (e.g., NaOH) at 60−80 °C.[1−3] The main advantages of alkali catalysts are their relatively low cost and capability of high biodiesel production rate. In such processes, biodiesel has to be washed to remove the contaminated traces of alkali. Bio-based oil feedstocks with free fatty acid content require the pretreatment with an acidic catalyst in order to reduce the subsequent soap formation (saponification) over alkali catalysts, which otherwise results in product loss and complicates the separation of biodiesel from the glycerol side product. The presence of water in the feedstock should be minimized as this can form fatty acids by the hydrolysis of triglycerides. Due to these pretreatment and purification steps, the alkali-catalyzed process can produce around 20 wt % wastewater as compared to the amount of biodiesel produced,[5] resulting in an energy-consuming and less environmentally friendly process.

Enzymatic synthesis of biodiesel using lipases as a catalyst is a greener alternative to the conventional alkali-catalyzed route,[6−12] which can be performed selectively under mild reaction conditions (20−50 °C). Lipases can directly convert triglycerides (by transesterification), fatty acids (by esterification), or mixtures thereof to biodiesel, without the need of the feedstock pretreatment. In such processes, no soaps are formed in the presence of water or fatty acids, so that lipases can be reused without requiring the additional product washing steps that generate wastewater. This particularly opens opportunities for biodiesel production by enzymatic conversion of bio-based oil feedstocks with relatively high fatty acid content (e.g., waste cooking oils).[13−15] Downsides of enzymes are that they are generally more expensive and have lower catalytic activity than conventional alkali catalysts, thus requiring longer reaction times to obtain the same product yields.[16] Lipases can be applied homogeneously as free enzymes or as heterogeneous catalysts immobilized on a solid support. Immobilized enzymes have been widely applied in the synthesis of biodiesel,[17] for example, by the (trans)esterification of waste cooking oils and ethanol.[18] The immobilization of enzymes has the advantages of increased catalyst stability, ease of reuse, and lower

Received: May 16, 2019
Revised: July 27, 2019
Accepted: July 30, 2019
Published: July 30, 2019

Downloaded via UNIV GRONINGEN on August 29, 2019 at 06:07:41 (UTC).
See https://pubs.acs.org/sharingguidelines for options on how to legitimately share published articles.

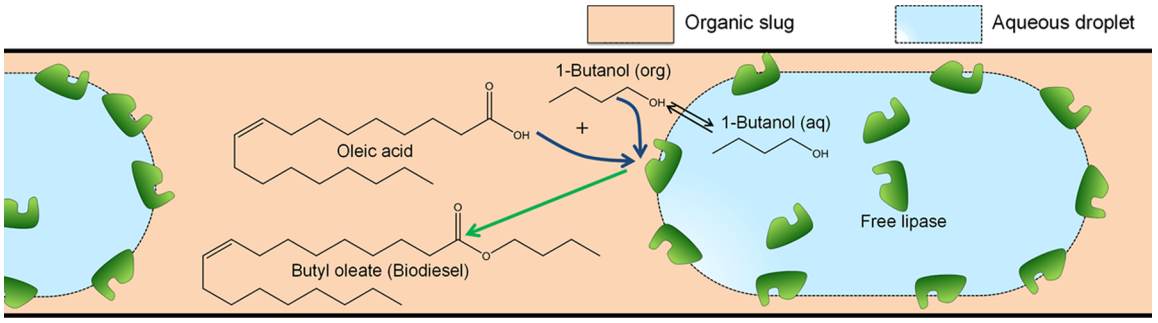

Figure 1. Graphical overview of the free lipase-catalyzed oleic acid esterification in a slug flow microreactor (conditions shown for a hydrophobic microreactor wall).

downstream processing costs as no additional catalyst separation is needed.[19] However, immobilized enzymes may be less active than free enzymes, and the immobilization procedure can be expensive and time-consuming. In contrast, by performing the free lipase-catalyzed (trans)esterification reactions in a biphasic aqueous−organic system with the enzyme in the aqueous phase and oil and biodiesel product in the organic phase (in the presence of a solvent), the lipase can be easily separated and reused. Furthermore, the separation of biodiesel (organic phase) from the glycerol byproduct (aqueous phase) in the case of transesterification of triglycerides is facilitated, although an excessive accumulation of glycerol in the lipase-containing aqueous phase may eventually affect the enzymatic performance. Moreover, such biphasic systems promote the enzyme performance of certain lipases by interfacial activation, where active sites are generated on the aqueous−organic interface by the induced lid-opening of the enzyme.[20−22] Hence, the free lipase-catalyzed reactions have been researched in biphasic aqueous−organic systems for the hydrolysis of triglycerides to fatty acids,[23−25] the esterification of fatty acids to biodiesel,[26−28] and the direct conversion of triglycerides to biodiesel by transesterification.[29,30] The reaction rate of oleic acid esterification with 1-butanol, as well as the transesterification of plant oils (i.e., sunflower oil with 1-butanol), in biphasic systems using the free *Rhizomucor miehei* lipase (RML) as a catalyst in batch reactors has been reported to be well described by a kinetic expression based on a Ping Pong Bi Bi mechanism with the competitive 1-butanol inhibition.[27,30] Enzyme performance was enhanced by an intensive stirring in these reactors, which increased the interfacial area and thus promoted the reaction. The remarkable influence of the interfacial area on the enzymatic reaction rate thus gives potential for process intensification in novel multiphase reactors in which a superior liquid−liquid interfacial area is achieved.

The potential of process intensification for biodiesel synthesis has been widely addressed and can increase the techno-economic feasibility of industrial-scale biodiesel production.[31,32] In this field, relatively few process intensification methods for enzymatic biodiesel synthesis have been reported so far. Continuous centrifugal contactor separator devices with intensified liquid−liquid mixing and combined reaction/separation have been applied for enzymatic biodiesel synthesis from both fatty acids and triglycerides using free or immobilized lipases.[33−35] Other works reported, for example, a perforated rotating disc reactor for the esterification of oleic acid with ethanol,[36] a basket impeller extractive reactor column for the transesterification of waste frying oil with ethanol (both using an immobilized lipase),[37] and a centrifugal partition reactor for the free lipase-catalyzed esterification of oleic acid with 1-butanol.[38,39] Continuous flow microreactors (chip- or capillary-based) have received a lot of attention in the synthesis of biodiesel using homogeneous or heterogeneous catalysts.[40−42] However, few studies have been performed on enzymatic biodiesel synthesis using immobilized[43−47] and free lipases in microreactors.[48,49] The transesterification of canola oil with methanol catalyzed by a lipase from *Candida rugosa* was performed in a capillary microreactor at 37 °C, where a fatty acid methyl ester (FAME biodiesel) yield of 72% was obtained in 120 min.[48] The esterification of oleic acid with ethanol using a lipase from *Candida antarctica* resulted in an almost 100% fatty acid conversion in 10 min in a Corning microreactor at 50 °C.[49]

Due to their small sizes (with characteristic dimensions on the order of ca. 1 mm or below), microreactors offer several fundamental advantages over traditional reactors (e.g., batch or continuous stirred tank reactors) such as enhanced heat transfer resulting in a precise temperature control to guarantee the optimal reaction activity.[50,51] The large specific interfacial area obtained in microreactors (e.g., operated under slug flow) enhances multiphase mass transfer so that chemical reactions with fast kinetics can be intensified considerably in microreactors.[52] Microreactors can provide high product quality consistency due to the narrowed residence time distribution in a continuous flow.[53] Furthermore, they allow for relatively easy upscaling by numbering-up without a significant performance loss (especially when the number of reaction channels involved is not very large).[54,55] Thus, microreactor flow processing holds great promises for an improved reaction performance for enzymatic biodiesel synthesis using free lipases, especially regarding a precise control of the large interfacial area available under slug flow.[56,57] The reduced shear stress in microreactors as compared to the rigorously stirred batch reactors may be critical to maintain a superior enzyme activity.

In this work, the homogeneous RML-catalyzed synthesis of butyl oleate (FABE biodiesel) was investigated by the esterification of oleic acid with 1-butanol (a bio-based alcohol that can be obtained from fermentation processes[58]). RML is a highly active free lipase that can synthesize biodiesel by the transesterification of triglycerides and esterification of fatty acids.[59] The biphasic aqueous−organic esterification of oleic acid using 1-butanol was reported to be faster than when using lower-molecular-weight alcohols (e.g., methanol, ethanol).[27] This is mainly because of the higher partition coefficient of 1-butanol over the two phases, which enhances the 1-butanol concentration in the organic phase and therewith increases the

DOI: 10.1021/acs.iecr.9b02693
Ind. Eng. Chem. Res. 2019, 58, 15432−15444

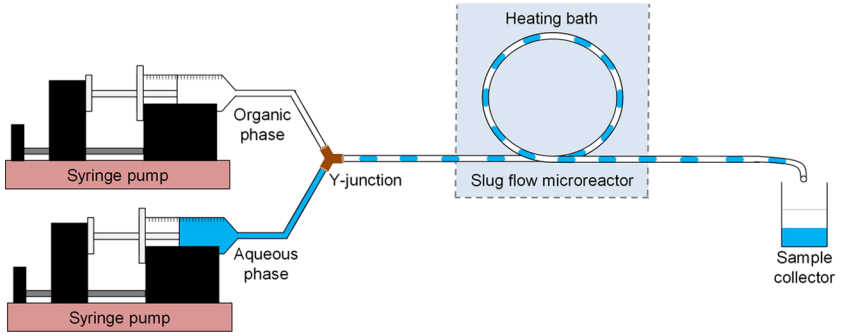

Figure 2. Schematic presentation of the PTFE microreactor setup (with syringe pumps typically used for fluid delivery).

kinetic reaction rate. The reaction was performed in a capillary microreactor system operated under slug flow. Here, the enzyme was dissolved in the aqueous phase, oleic acid in the organic (*n*-heptane) phase, and 1-butanol distributed over the two phases with the reaction taking place on the aqueous–organic interface (Figure 1). Process parameters (i.e., length, diameter, and material of microreactors, two-phase flow rates, enzyme and substrate concentrations) were varied to investigate the reaction performance to examine the validity and applicability of the literature kinetic model in slug flow microreactors and identify the intensification potential therein by further performance optimization.

2. EXPERIMENTAL SECTION

2.1. Chemicals. Oleic acid (technical grade, 90%), 1-butanol (99%), ethyl oleate (98%), *Rhizomucor miehei* lipase in the aqueous solution (≥ 20,000 unit g^{-1}), *N*-methyl-*N*-(trimethylsilyl)trifluoroacetamide for GC derivatization (98.5%), pentadecane (99%), and buffer compounds ($Na_2HPO_4{\cdot}2H_2O$ (98.0%) and KH_2PO_4 (>99%)) were obtained from Sigma-Aldrich. Acetic acid (99.5%) and *n*-heptane (99%) were obtained from Acros Organics. For the preparation of aqueous solutions, Milli-Q water was used. The aqueous *Rhizomucor miehei* lipase (RML) solution had a density of 1.131 g mL^{-1}, corresponding to a dry enzyme concentration ($C_{enz,aq}$) of ca. 131 g L_{aq}^{-1}.

2.2. Microreactor Setup and Experimental Procedure. Figure 2 depicts the experimental setup. The aqueous feed consisted of RML (0.5–5 g L_{aq}^{-1}) diluted in a phosphate buffer solution (pH 5.6). The organic feed consisted of 1-butanol (0.25–4 mol L_{org}^{-1}) and oleic acid (0.15–1.3 mol L_{org}^{-1}) in *n*-heptane including pentadecane (0.1 mol L_{org}^{-1}) as an in situ internal standard. In most experiments, the two phases were fed by syringe pumps (model LA30, HLL GmbH) into a polyether ether ketone (PEEK) Y-junction (inner diameter: 0.5 mm), generating an aqueous–organic slug flow in the subsequent microreactor made of polytetrafluoroethylene (PTFE). For a few experiments aiming at reaching almost a full conversion of oleic acid at sufficiently long residence times (30–60 min), a binary HPLC pump from Hewlett Packard (Agilent series 1100) was used to feed both liquid phases. All experiments were performed at atmospheric pressure and ca. 30 °C, which is within the optimum performance temperature (30–50 °C) for ester synthesis by the *Rhizomucor miehei* lipase (www.novozymes.com). In the free RML-catalyzed transesterification of sunflower oil with methanol, it was found that highest biodiesel yield was obtained at 30–40 °C, and the yield was significantly lower at 50–60 °C, probably due to the enzyme deactivation.[29] The microreactor was heated by immersing it in a heated water bath. Throughout the experiments, PTFE microreactors of different lengths (L_C = 0.5–8 m) and inner diameters (d_C = 0.3–1 mm) were typically used. The volumetric flow rates of the aqueous (Q_{aq}) and organic (Q_{org}) phases ranged from 0.007 to 0.1 mL min^{-1} and 0.02 to 0.1 mL min^{-1}, respectively. In the experiments, the liquid–liquid flow pattern in the microreactor was captured with a Nikon D3300 digital camera equipped with a Nikon lens (AF-S Micro NIKKOR 60 mm F/2.8G ED). At the outlet of the microreactor, the reaction mixture was quenched with acetic acid to deactivate the enzyme and stop the reaction. The sample mixture was then centrifuged to separate the organic phase for product analysis (vide infra).

To investigate the effect of microreactor wettability on the reaction performance, several experiments were performed in a hydrophilic stainless steel (SS) capillary microreactor (L_C = 1 m, d_C = 1 mm). The two phases were mixed in a stainless steel T-junction (inner diameter: 1.5 mm). The volumetric flow rates of the aqueous and organic phases ranged from 0.007 to 0.1 mL min^{-1} and 0.02 to 0.1 mL min^{-1}, respectively. To indicate slug flow patterns in this nontransparent microreactor, a glass capillary (L_C = 10 mm, d_C = 1 mm) was attached at the microreactor outlet by a stainless steel connector to allow for flow visualization therein. The other experimental details remain unchanged.

All experimental data were collected under a steady-state operation in the microreactor. It is assumed that a steady state was achieved by waiting at least three times the residence time under a stable slug flow operation. Each experimental condition was performed at least in triplicate.

2.3. Analysis. Substrate and product concentrations in the organic phase before and after the reaction were analyzed by a gas chromatograph equipped with flame ionization detector (GC-FID). Samples were prepared by diluting 5–20 μL of the collected organic phase in 1.8 mL of *n*-heptane followed by adding 20 μL of *N*-methyl-*N*-(trimethylsilyl)trifluoroacetamide (MSTFA) for the derivatization of oleic acid by silylation. GC-FID analysis was performed with a Restek Stabilwax-DA column (15 m × 0.32 mm × 0.25 μm), where its temperature was increased from 50 to 300 °C at 50 °C min^{-1} using helium carrier gas at 2.5 mL min^{-1}. Calibration measurements using standard solutions were performed to determine the relative response factors of (silylated) oleic acid and butyl oleate. Since butyl oleate was not available in a pure form, calibration was performed for ethyl oleate assuming an equal relative response factor by correcting for the difference in the molecular weight.[60]

DOI: 10.1021/acs.iecr.9b02693
Ind. Eng. Chem. Res. 2019, 58, 15432–15444

2.4. Definitions. The oleic acid conversion (X_{FA}) and butyl oleate yield (Y_{FABE}) in the microreactor are determined as follows

$$X_{FA} = \left(1 - \frac{C_{FA,org}}{C_{FA,org,0}}\right) \times 100\% \quad (1)$$

$$Y_{FABE} = \frac{C_{FABE,org}}{C_{FA,org,0}} \times 100\% \quad (2)$$

Here, $C_{FA,org}$ and $C_{FABE,org}$ are the concentrations of oleic acid and butyl oleate (FABE), respectively, in the organic phase at a certain microreactor axial position. $C_{FA,org,0}$ is the oleic acid concentration in the organic phase at the microreactor inlet.

The residence time (τ) in the microreactor is calculated by

$$\tau = \frac{V_C}{Q_M} = \frac{\frac{\pi}{4} d_C^2 L_C}{Q_{org} + Q_{aq}} \quad (3)$$

where V_C, d_C, and L_C are the microreactor volume, inner diameter, and length, respectively. Q_M denotes the total volumetric flow rate of the aqueous−organic mixture.

The mixture velocity (U_M) is thus defined as

$$U_M = \frac{Q_M}{\frac{\pi}{4} d_C^2} = \frac{Q_{org} + Q_{aq}}{\frac{\pi}{4} d_C^2} \quad (4)$$

3. RESULTS AND DISCUSSION

3.1. Reaction Performance in the PTFE Microreactor.

3.1.1. Typical Reaction Profile. A typical reaction profile in the PTFE microreactor as a function of the residence time is presented in Figure 3. The residence time was altered by performing the reaction in microreactors of different lengths for a given total flow rate. The reaction variables (i.e., enzyme and substrate concentrations) and the aqueous-to-organic flow ratios were kept constant, so that flow patterns did not change significantly for these different experiments. No unidentified side products were observed from the GC-FID analysis, and the sum of oleic acid and butyl oleate corresponded to a closed mass balance for each residence time (Figure 3), indicating that all reacted oleic acid was converted to butyl oleate.

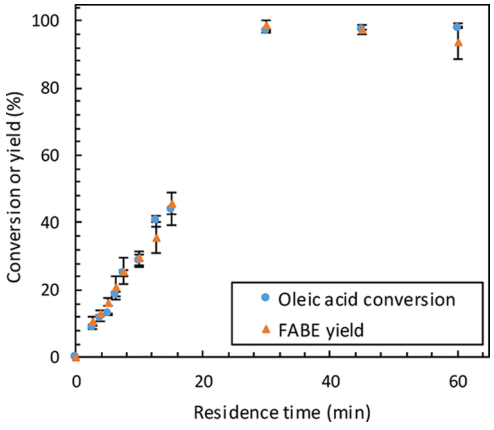

Figure 3. Measured oleic acid conversion and butyl oleate yield as a function of the residence time in the PTFE microreactor. Reaction conditions: 30 °C, $C_{BuOH,org,f}$ = 0.96 mol L_{org}^{-1} (i.e., the concentration of 1-butanol in the organic feed), $C_{FA,org,0}$ = 0.62 mol L_{org}^{-1}, $C_{enz,aq}$ = 2.32 g L_{aq}^{-1}, d_C = 0.8 mm, L_C = 1.67−10 m, and $Q_{aq} = Q_{org}$ = 0.05 mL min^{-1} for τ < 30 min; experiments for τ = 30−60 min were conducted in a 10 m microreactor by adjusting the flow rate (Q_{aq}/Q_{org} = 1). Error bar indicates the standard deviation measured from the experimental runs at least in triplicate (the same for other figures hereafter, if applicable).

The oleic acid conversion and butyl oleate yield appeared to be proportional to the residence time for a given flow rate (i.e., at τ < 30 min). A 46% oleic acid conversion was obtained in 15 min in this PTFE microreactor (d_C = 0.8 mm) at the given operating conditions. Further increasing the residence time to 30 min and higher resulted in nearly full oleic acid conversion and butyl oleate yield (96−98%). It should be noted that the experiments at residence times of 30−60 min were conducted using a binary HPLC pump instead of syringe pumps for the rest of the experiments (cf. Section 2.2). This pump switch seemed to cause a slightly different slug flow profile with a somewhat higher liquid−liquid interfacial area (4125 m^2 m^{-3}) than those at other conditions shown in this figure (3700 m^2 m^{-3}). This higher interfacial area contributed to a higher reaction rate, and thus a more than doubled conversion of oleic acid (close to 100%) was achieved at 30 min compared with that at 15 min. The effect of the interfacial area (and its calculation) on the reaction performance will be addressed in more detail in Section 3.1.3.

3.1.2. Absence of Mass Transfer Limitations. Experiments were performed under different mixture velocities (U_M; cf. eq 4) in the PTFE microreactor to determine if there were mass transfer limitations for this reaction (Figure 4). The residence time was kept equal for a given mixture velocity by adjusting the microreactor length (the aqueous-to-organic flow ratio being kept the same). It is commonly known that, under slug flow, a relatively high mixture velocity results in an increased mass transfer coefficient (k_L) in both the organic slug ($k_{L,org}$) and the aqueous droplet ($k_{L,aq}$).[61−63] Thus, under mass transfer limited conditions, the reaction rate would be affected by a significant change in the mixture velocity (or k_L). The results in Figure 4 suggest that, under the conditions of this work, a considerable influence of the mixture velocity on the oleic acid conversion is absent for a given residence time. Thus, it is reasonable to conclude that the reaction in the current microreactor system was limited by the slow reaction kinetics

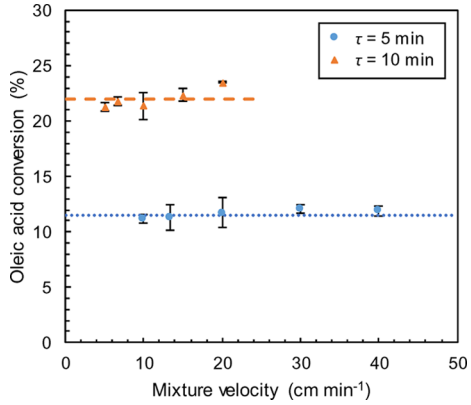

Figure 4. Influence of the mixture velocity on the measured oleic acid conversion in the PTFE microreactor. Reaction conditions: 30 °C, $C_{BuOH,org,f}$ = 0.96 mol L_{org}^{-1}, $C_{FA,org,0}$ = 0.62 mol L_{org}^{-1}, $C_{enz,aq}$ = 2.32 g L_{aq}^{-1}, d_C = 0.8 mm, Q_{aq}/Q_{org} = 1, and τ = 5 or 10 min. Lines are shown for visual guidance.

DOI: 10.1021/acs.iecr.9b02693
Ind. Eng. Chem. Res. 2019, 58, 15432−15444

of the enzymatic reaction as also supported by the superior mass transfer properties of slug flow microreactors. In other words, mass transfer effects related to the transport of substrates and enzyme to the liquid−liquid interface (the locus of the reaction) on the overall reaction rate can be neglected.[27]

The small deviations observed in the oleic acid conversion in Figure 4, especially at the longer residence time (τ = 10 min), could be due to a slight change in the aqueous−organic slug flow profile. For experiments with each capillary microreactor of a certain length (Figure 2), the reactor was reconnected to the PEEK Y-junction, which can result in a slight alteration in the mixer geometry.[64,65] The capillary might be also slightly different in terms of wettability or roughness. The flow rate, and thus the flow ratio between the two phases, could change slightly due to pump fluctuations and inaccuracies. All these factors could have a certain influence on the liquid−liquid interfacial area that led to a slightly different oleic acid conversion (see more details of the interfacial area effect in the following sections).

3.1.3. Influence of the Liquid−Liquid Interfacial Area. The lipase catalyzed biphasic (esterification) reaction is well known to be affected by the liquid−liquid interfacial area in biphasic systems, which has been reported extensively.[66−68] In reported kinetic studies,[27,39] it was concluded that the reaction rate of the free RML-catalyzed esterification of oleic acid with 1-butanol in a biphasic aqueous−organic system is influenced by the aqueous−organic interfacial area. However, in these studies, no dedicated experiments were performed to quantify the effect of the interfacial area on the reaction rate. Furthermore, it was difficult to visualize all droplets, for example, in the batch reactor setup, which, in addition to the non-uniform droplet size distribution, could complicate the accurate determination of the interfacial area. In a continuous flow microreactor, a well-defined slug flow with uniform slug and droplet sizes can be easily generated. Thus, the interfacial area can be determined precisely by flow visualization. To clearly reveal the influence of the interfacial area, experiments were performed in PTFE microreactors with different inner diameters. For each microreactor (L_C = 1 m), the mixture velocity was kept constant (U_M = 20 cm min^{-1}) by adjusting the total volumetric flow rate at a residence time of 5 min (Q_{aq}/Q_{org} = 1). The oleic acid conversion increased with decreasing microreactor diameter due to the increase of the interfacial area generated in smaller microreactors (Figure 5). Given that there were no mass transfer limitations in microreactors with an inner diameter of 0.8 mm (Figure 4), it can be assumed that these are also absent in microreactors of similar inner diameters operated under the same mixture velocity (as shown in Figure 5), which holds especially in the smaller diameter microreactors where mass transfer is further enhanced by the increase in the interfacial area therein. The results in Figure 5 clearly confirm that the reaction kinetic rate is positively affected by the interfacial area in PTFE microreactors. An in-depth discussion of this effect is given in Section 3.2.

The interfacial area (as shown in Figure 5) was calculated according to the flow images captured (e.g., see Figure 6) and using the equations shown below. The droplet and slug lengths (denoted as L_D and L_S, respectively) in the slug flow images were measured (Figure 6). The total specific interfacial area (a) available for the reaction can be distinguished between the contributions from the cap (a_{cap}) and film (a_{film}) regions.

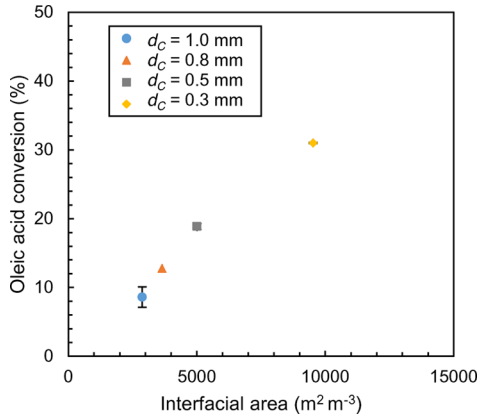

Figure 5. Influence of the interfacial area on the measured oleic acid conversion in PTFE microreactors of different inner diameters. Reaction conditions: 30 °C, U_M = 20 cm min^{-1}, $C_{BuOH,org,f}$ = 0.96 mol L_{org}^{-1}, $C_{FA,org,0}$ = 0.62 mol L_{org}^{-1}, $C_{enz,aq}$ = 2.32 g L_{aq}^{-1}, d_C = 0.3−1 mm, L_C = 1 m, and τ = 5 min.

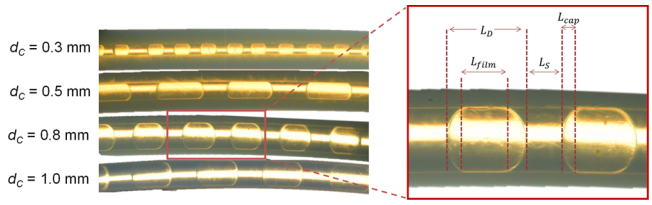

Figure 6. Slug flow pictures in PTFE microreactors of different inner diameters, including a magnified view of the droplet and slug dimensions. The aqueous phase appeared as the droplet and the organic phase as the slug.

$$a = a_{cap} + a_{film} \tag{5}$$

The liquid film surface (or the droplet body) is assumed to be cylinder-shaped with a droplet diameter (d_D) approximately equal to d_C and a film length of L_{film}. Thus, it is obtained that

$$a_{film} = \frac{\pi d_C L_{film}}{\frac{\pi}{4} d_C^{\,2}(L_D + L_S)} = \frac{4L_{film}}{d_C(L_D + L_S)} \tag{6}$$

The end cap is assumed to be of the oblate spheroid shape with three elliptic radii being approximated as $d_C/2$, $d_C/2$, and L_{cap} (Figure 6). Thus, there is

$$a_{cap} = \frac{\frac{\pi}{2} d_C^{\,2} + \pi \frac{L_{cap}^{\,2}}{e} \ln\left(\frac{1+e}{1-e}\right)}{\frac{\pi}{4} d_C^{\,2}(L_D + L_S)} \tag{7}$$

where e is the ellipticity of the oblate spheroid and defined as

$$e = \sqrt{\frac{\left(\frac{d_C^{\,2}}{4}\right) - L_{cap}^{\,2}}{\left(\frac{d_C^{\,2}}{4}\right)}} \tag{8}$$

In PTFE microreactors operated under slug flow in this work, a was varied between 2500 and10,000 m^2 m^{-3}. A higher a was obtained in smaller diameter microreactors or at higher aqueous-to-organic volumetric flow ratios. In the literature, an even higher interfacial area has been reported for the same reaction system. For instance, in the rigorously stirred batch reactor (at 1500 rpm) reported by Kraai et al.,[27] nearly 100% oleic acid conversion was achieved under similar conditions

DOI: 10.1021/acs.iecr.9b02693
Ind. Eng. Chem. Res. 2019, 58, 15432−15444

using a lower lipase concentration ($C_{enz,aq}$ = 0.2 g L_{aq}^{-1}). This higher enzyme activity in the batch reactor was due to a very high liquid−liquid interfacial area by the fine organic droplets (average Sauter diameter of 24 μm) generated therein, corresponding to a specific interfacial area of 105,000 m^2 m^{-3} (cf. Section 1 in the Supporting Information for calculation details).[27] Although higher interfacial areas, and thus reaction rates, could be obtained in an optimized laboratory-scale batch reactor under intensive stirring than in the microreactor used in this work, much higher energy consumption was also involved in the former case. Also, it is expected that, for pilot or industrial scale batch setups, the effective aqueous−organic interfacial area can decrease drastically, negatively affecting the reaction performance given the scale-dependent mixing property.[69,70] For instance, in laboratory-scale liquid−liquid agitators (10 cm in diameter), a values of ca. 3000−8000 m^2 m^{-3} were obtained, and a drastic decrease in a was observed when further increasing the vessel diameter.[70] In contrast, microreactors have the benefit of continuous flow operation and relatively easy upscaling without a significant performance loss (e.g., in the effective interfacial area). Upscaling of microreactors can be done by numbering-up, where multiple microreactors are operated simultaneously as a reactor bundle.[54] When a proper distributor is attached before the individual reactor inlets, the liquid−liquid slug flow profile can be generated more or less uniformly across different channels so that the enhanced mass transfer and process control in scaled-up microreactors systems is not changed considerably.[55] Moreover, when operating the reaction in smaller diameter microreactors where the aqueous−organic interfacial area is further increased, the reaction rate can be enhanced even further (e.g., a full oleic acid conversion can be thus achieved at shorter residence times or lower enzyme concentrations). However, this efficiency increase might be at the cost of increased numbering-up efforts since more reaction channels are likely required for a given production capacity.

3.2. Kinetic Model Validation in the PTFE Microreactor. From the previous studies,[27,39] it was concluded that the kinetics of the enzymatic esterification of oleic acid with 1-butanol could be well described by a Ping Pong Bi Bi mechanism with competitive inhibition of 1-butanol. Similar mechanisms were found in the lipase-catalyzed (trans)-esterification of other fatty acids (or plant oils) and alcohols.[26,30,71] Such mechanism describes that the substrates are adsorbed successively to the enzyme active site on the liquid−liquid interface. The reaction rate of oleic acid (R_{FA}) is given as[27]

$$R_{FA} = -\frac{k_{enz}C_{enz,aq}}{1 + \left(\frac{K_{M,FA}}{C_{FA,org}}\right)\left(1 + \left(\frac{C_{BuOH,org}}{K_{I,BuOH}}\right)\right) + \left(\frac{K_{M,BuOH}}{C_{BuOH,org}}\right)} \quad (9)$$

Here, $C_{enz,aq}$ is the aqueous phase enzyme concentration (g_{enz} L_{aq}^{-1}). $C_{FA,org}$ and $C_{BuOH,org}$ denote the molar concentrations of fatty acid (oleic acid in this case) and 1-butanol in the organic phase, respectively. k_{enz} is the kinetic constant (mol L_{aq} g_{enz}^{-1} L_{org}^{-1} s^{-1}). $K_{M,FA}$ and $K_{M,BuOH}$ are the Michaelis−Menten parameters for oleic acid and 1-butanol, respectively, and $K_{I,BuOH}$ is the inhibition parameter of 1-butanol.

According to the mass balance in the microreactor, it is obtained that

$$Q_{org}\frac{dC_{FA,org}}{dV_C} = R_{FA} \quad (10)$$

The above equation is rearranged as

$$\frac{Q_{org}}{Q_{org} + Q_{aq}}\frac{dC_{FA,org}}{d\tau} = R_{FA} \quad (11)$$

The distribution of 1-butanol over the water−n-heptane system is well described by assuming a partition coefficient (m = 1.83 at 30 °C),[72] which is unaffected by the amount of oleic acid or 1-butanol present in the system.[27]

$$m = \frac{C_{BuOH,org}}{C_{BuOH,aq}} \quad (12)$$

Here, $C_{BuOH,aq}$ is the molar concentration of 1-butanol in the aqueous phase. $C_{BuOH,org}$ at a certain microreactor axial position is then derived according to its mass balance as

$$C_{BuOH,org} = \frac{C_{BuOH,org,f} - (C_{FA,org,0} - C_{FA,org})}{1 + \frac{Q_{aq}}{mQ_{org}}} \quad (13)$$

The literature has indicated that the enzymatic reaction takes place at the aqueous−organic interface;[27,66,67] thus, the reaction rate is affected greatly by the interfacial area (e.g., see Figure 5) and the corresponding amount of enzyme available at the interface. According to the enzyme mass balance, there is[73]

$$C_{enz,aq} = C_{enz,bulk} + E^*a\left(1 + \frac{Q_{org}}{Q_{aq}}\right) \quad (14)$$

where E^* is the superficial concentration of enzyme adsorbed on the aqueous−organic interface (g_{enz} m^{-2}) and $C_{enz,bulk}$ is the unbound enzyme concentration in the liquid bulk, which is described by

$$C_{enz,bulk} = \frac{K_d^*E^*}{E_{max}^* - E^*} \quad (15)$$

E_{max}^* is the maximum superficial concentration of the adsorbed enzyme (g_{enz} m^{-2}) and K_d^* is the interfacial affinity constant (g_{enz} L_{aq}^{-1}) that describes the equilibrium between the enzyme adsorption/desorption rate. This indicates the existence of a dynamic exchange between enzymes at the interface and in the bulk.

Equation 14 is also based on the assumption that the actual phase fraction in the microreactor is equal to the volumetric phase fraction (e.g., β_{org} for the organic phase as defined in eq 16), which is roughly satisfied for the liquid−liquid slug flow at low mixture velocities as used in this work (i.e., with negligible film thickness)[74]

$$\beta_{org} = \frac{Q_{org}}{Q_{aq} + Q_{org}} \quad (16)$$

When the majority of the enzyme is assumed unbound and present in the aqueous bulk (e.g., when $C_{enz,aq}$ is not too low), there is

DOI: 10.1021/acs.iecr.9b02693
Ind. Eng. Chem. Res. 2019, 58, 15432−15444

$$C_{enz,bulk} \gg E^* a\left(1 + \frac{Q_{org}}{Q_{aq}}\right) \quad (17)$$

Thus, $C_{enz,aq} \approx C_{enz,bulk}$. With the presence of a sufficiently large interfacial area available for the enzyme to adsorb, the interface is not fully saturated by the adsorbed enzyme (i.e., when $E^*_{max} \gg E^*$). Then, according to eq 15, $C_{enz,\,bulk} \propto E^*$, and consequently $C_{enz,\,aq} \propto E^*$. This first implies that, under such circumstances, E^* would remain constant for a given $C_{enz,\,aq}$. Moreover, an increase in the interfacial area would lead to a linear increase in the absolute amount of enzyme adsorbed at the interface, and with that the reaction rate. Then, eq 9 can be rewritten as a function of the interfacial area for the current microreactor system as

$$R_{FA} = R''_{FA} a\left(1 + \frac{Q_{aq}}{Q_{org}}\right) = -\frac{k''_{enz} a\left(1 + \frac{Q_{aq}}{Q_{org}}\right) C_{enz,aq}}{1 + \left(\frac{K_{M,FA}}{C_{FA,org}}\right)\left(1 + \left(\frac{C_{BuOH,org}}{K_{I,BuOH}}\right)\right) + \left(\frac{K_{M,BuOH}}{C_{BuOH,org}}\right)} \quad (18)$$

where R''_{FA} is the reaction rate of oleic acid based on the interfacial area[27] and k''_{enz} is the kinetic constant based on the interfacial area. The value of k''_{enz} should be constant and is determined from the literature, that is, by correcting k_{enz} for the estimated interfacial area in the batch reactor studied by Kraai et al.[27] (cf. Section 1 in the Supporting Information). Values of kinetic parameters in eq 18 according to their study are further presented in Table 1.

Table 1. Values of the Kinetic Parameters in eq 18[a]

parameter	value
k_{enz} ($\times 10^{-3}$ mol L_{aq} g_{enz}^{-1} L_{org}^{-1} s^{-1})	7.384
k''_{enz} ($\times 10^{-8}$ mol m g_{enz}^{-1} s^{-1})[b]	2.956
$K_{M,FA}$ (mol L_{org}^{-1})	0.06776
$K_{M,BuOH}$ (mol L_{org}^{-1})	0.2536
$K_{I,BuOH}$ (mol L_{org}^{-1})	0.1277

[a]Adapted from the model of Kraai et al.[27] with permission from Elsevier. [b]Details of calculation are shown in Section 1 of the Supporting Information.

Equation 11, in combination with eqs 13 and 18, can be solved analytically to obtain the relation between the oleic acid conversion and the residence time in the microreactor based on the specific interfacial area obtained by flow visualization and the kinetic parameters in Table 1 (cf. Eq. S17 in the Supporting Information). The positive effect of the interfacial area on the oleic acid conversion as observed in Figure 5 can be further explained according to this relation.

To validate the applicability of the kinetic model of Kraai et al.[27] (eq 18 with the kinetic parameters from Table 1) in the current microreactors, the experimental and modeled oleic acid conversions are depicted as a function of the residence time in PTFE microreactors of 0.5 and 0.8 mm inner diameters (Figure 7).

The kinetic model of Kraai et al.[27] is able to well describe the oleic acid conversion in the PTFE microreactor when correcting for the difference in the liquid−liquid interfacial area obtained therein. A somewhat significant error of the oleic

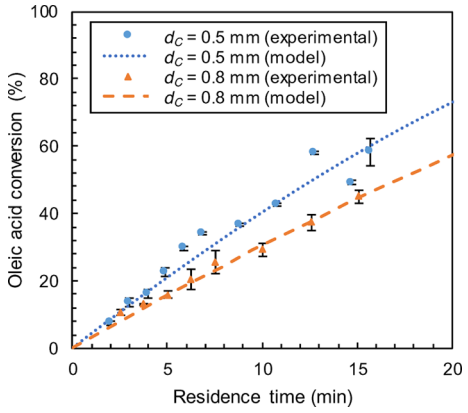

Figure 7. Oleic acid conversion as a function of the residence time in PTFE microreactors according to the experimental measurement and the kinetic model of Kraai et al.[27] Reaction conditions: 30 °C, U_M = 20 cm min^{-1}, Q_{aq}/Q_{org} = 1, $C_{FA,org,0}$ = 0.62 mol L_{org}^{-1}, $C_{BuOH,org,f}$ = 0.96 mol L_{org}^{-1}, $C_{enz,aq}$ = 2.32 g L_{aq}^{-1}, and d_C = 0.5 or 0.8 mm. The residence time was varied by changing the microreactor length. a is about 5000 or 3700 m^2 m^{-3} for the microreactor with d_C = 0.5 or 0.8 mm, respectively.

acid conversion in the experimental values seems to exist at long residence times. This could be due to the increased pressure drop given the long microreactors used, which may result in fluctuation in the flow rate delivered by the syringe pump and/or flow profile disturbances, thus affecting the effective residence time or interfacial area.

To further validate the model for a broader range of reaction conditions, kinetic variables (i.e., the aqueous enzyme concentration, initial 1-butanol and oleic acid concentrations in the organic feed) were varied, and the obtained experimental results are compared with the model predictions in Figure 8a−c. All reactions were performed in a PTFE microreactor (d_C = 0.8 mm, L_C = 1 m) at the same flow conditions (Q_{aq} = 0.05 mL min^{-1}, Q_{org} = 0.05 mL min^{-1}, and τ = 5 min). The model in general corresponds well with the experimental data. The reaction rate appears to be linearly dependent on the aqueous phase enzyme concentration and thus is enhanced if there is more enzyme available to be bound to the aqueous−organic interface (Figure 8a). This further confirms our previous assumption that the aqueous enzyme concentration is indeed proportional to the superficial concentration of enzyme adsorbed on the aqueous−organic interface (i.e., $C_{enz,\,aq} \propto E^*$) for the experiments described in this work.

Figure 8b reveals that, for relatively low 1-butanol concentrations in the organic feed ($C_{BuOH,org,f}$), the reaction rate increased to an optimum, and further increasing the concentration led to a decrease in the reaction rate. This indicates that although increasing the 1-butanol concentration could enhance the reaction rate, 1-butanol tended to compete with oleic acid for the enzyme active sites and thus competitively inhibited the reaction.[27] A decrease in the initial oleic acid concentration ($C_{FA,org,0}$) resulted in a lower oleic acid conversion (Figure 8c), since the reaction could be roughly assumed below first order in oleic acid (cf. Eq. S10 in the Supporting Information).

Experiments were performed in the PTFE microreactor at various volumetric organic fractions (β_{org}; eq 16) by varying the aqueous-to-organic volumetric flow ratio. The oleic acid conversion decreased all the way with increasing β_{org} (or

DOI: 10.1021/acs.iecr.9b02693
Ind. Eng. Chem. Res. 2019, 58, 15432−15444

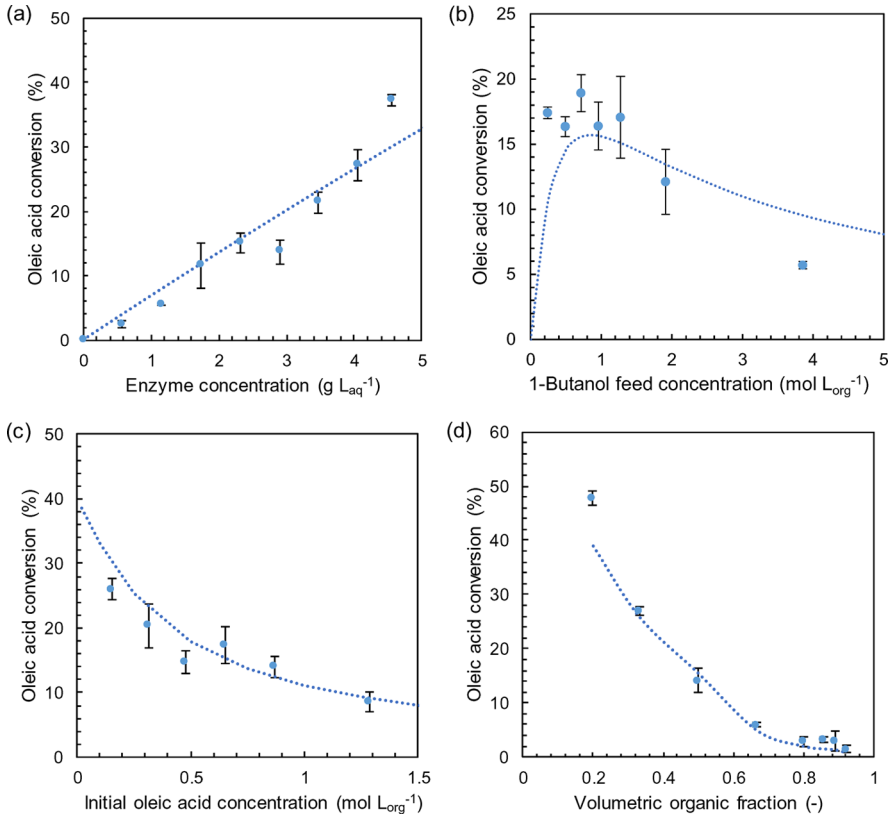

Figure 8. Influence of the (a) enzyme concentration, (b) 1-butanol feed concentration, (c) initial oleic acid concentration, and (d) volumetric organic fraction on the oleic acid conversion in a PTFE microreactor according to the experimental measurements and the kinetic model of Kraai et al.[27] Reaction conditions (unless stated otherwise): 30 °C, Q_M = 0.1 mL min^{-1}, Q_{aq}/Q_{org} = 1, $C_{FA,org,0}$ = 0.62 mol L_{org}^{-1}, $C_{BuOH,org,f}$ = 0.96 mol L_{org}^{-1}, $C_{enz,aq}$ = 2.32 g L_{aq}^{-1}, d_C = 0.8 mm, L_C = 1 m, and τ = 5 min. Lines illustrate the model predictions, and symbols represent the measured data. $a \approx 3700$ m^2 m^{-3} for Q_{aq}/Q_{org} = 1.

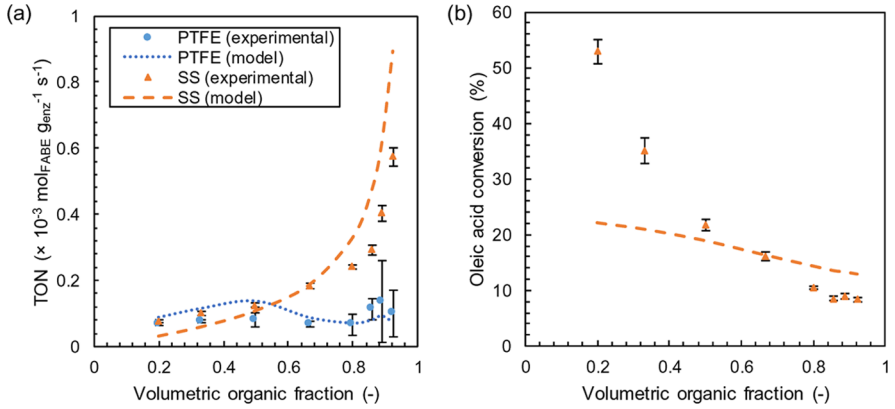

Figure 9. Influence of the volumetric organic fraction on the (a) enzyme turnover number and (b) oleic acid conversion. Data in (a) are shown for both the PTFE microreactor (d_C = 0.8 mm, L_C = 1 m, and τ = 5 min) and the stainless steel microreactor (d_C = 1.0 mm, L_C = 1 m, and τ = 7.8 min). Data in (b) are shown only for the same stainless steel microreactor. Reaction conditions: 30 °C, Q_M = 0.1 mL min^{-1}, $C_{BuOH,org,f}$ = 0.96 mol L_{org}^{-1}, $C_{FA,org,0}$ = 0.62 mol L_{org}^{-1}, and $C_{enz,aq}$ = 2.32 g L_{aq}^{-1}. Lines illustrate the kinetic model predictions, and symbols represent the measured data.

equivalently with increasing Q_{aq}/Q_{org}), which is in good agreement with the model predictions as well (Figure 8d). This oleic acid conversion decrease is first due to the increase in the volume of the organic reaction phase, which logically resulted in relatively lower conversions since the reaction that is below first order in oleic acid. Above that, an increase in the volumetric organic fraction led to longer organic slugs, which are the continuous phase in the hydrophobic PTFE microreactor (Figure 6), meaning that less and smaller aqueous droplets were formed for a given volume of the unit cell in slug flow. This resulted in a decreased specific interfacial area and, with that, oleic acid conversion.

The kinetic model of Kraai et al.[27] was originally developed for a fixed interfacial area (albeit a non-uniform droplet size distribution) in a batch reactor, since the stirring speed and the aqueous-to-organic volumetric ratios were not altered. The results in this work (Figures 7 and 8)) corroborate the model validity in the current PTFE microreactor system under wider operational ranges dealing with different aqueous-to-organic volumetric flow ratios and interfacial areas thereof.

DOI: 10.1021/acs.iecr.9b02693
Ind. Eng. Chem. Res. 2019, 58, 15432−15444

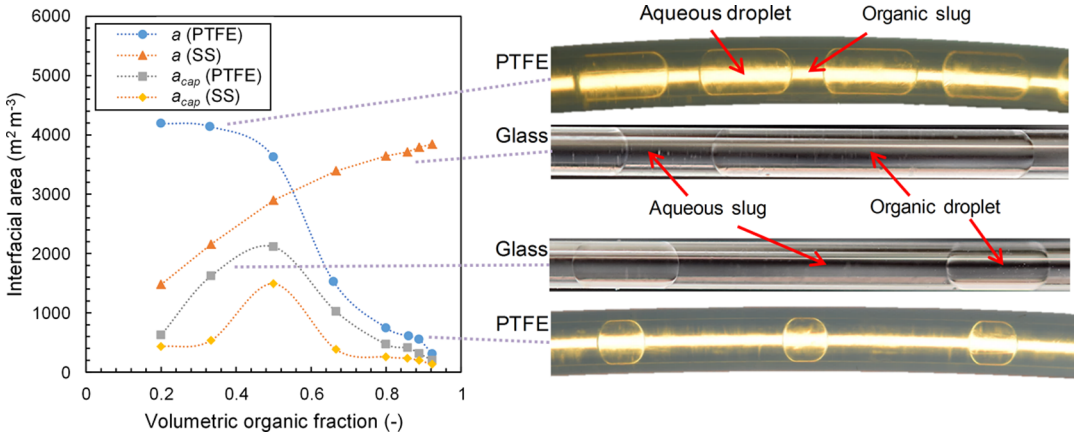

Figure 10. Effect of the volumetric organic fraction on the measured interfacial area in the hydrophobic PTFE and hydrophilic stainless steel capillary microreactors. Typical flow images are included for illustrative purposes. The interfacial area in the stainless steel microreactor was inferred from the flow images in the glass capillary attached at its outlet.

3.3. Biodiesel Production Optimization: Enzyme Turnover Number in PTFE and Stainless Steel Microreactors. Enzymatic biodiesel synthesis in biphasic systems can be economically attractive as it greatly reduces the required reaction temperature and processing steps. However, the main downside of using enzymes industrially for this application is that lipases are more expensive than conventional alkali catalysts and confined by relatively slow reaction kinetics. Hence, to increase the techno-economic feasibility of the process, enzyme utilization needs to be optimized. The enzyme turnover number (TON) is a good indicator for the enzyme usage efficiency and process performance, which is defined as the amount of biodiesel (in this case butyl oleate) produced per amount of enzyme per unit time.

$$\mathrm{TON} = \frac{Q_{org} C_{FA,org,0} Y_{FABE}}{Q_{aq} C_{enz,aq} \tau} \tag{19}$$

Under operating conditions with high TON values, less enzyme is required for a target production capacity, which significantly increases the economic feasibility of the process.

To optimize the PTFE microreactor for more efficient enzyme usage, the aqueous-to-organic volumetric flow ratio was already altered in the hydrophobic PTFE reactor (Figure 8d). The corresponding experiments were also performed in a hydrophilic stainless steel (SS) microreactor. Each experiment was carried out under otherwise the same conditions (i.e., temperature, enzyme, and initial substrate concentrations) at a residence time of 5 min in the PTFE (d_C = 0.8 mm) and 7.8 min in the stainless steel microreactor (d_C = 1 mm). The reaction performance of the stainless steel microreactor is compared with that of the PTFE microreactor in terms of TON (Figure 9a) and with the model prediction in terms of the oleic acid conversion (Figure 9b). It is seen that by performing the reaction at higher β_{org} values (i.e., lower Q_{aq}/Q_{org} values) in the stainless steel microreactor, a higher TON value is obtained (Figure 9a). For the PTFE microreactor, however, higher β_{org} values do not always contribute to an increase in TON. This is because an increase in β_{org}, in this case, resulted in a decrease in the interfacial area, thus decreasing the reaction rate. So, although less enzyme was required, the decreased reaction rate counteracted in such a way that TON is more or less unaffected at different volumetric organic fractions.

By adjusting Q_{aq}/Q_{org} and thus β_{org}, the concentrations of 1-butanol in the aqueous and organic phases in the microreactor were altered according to its distribution over the two phases (eq 13). However, this change in concentration (e.g., $C_{BuOH,org,0}$ = 0.3 mol L_{org}^{-1} for Q_{aq}/Q_{org} = 4 and $C_{BuOH,org,0}$ = 0.92 mol L_{org}^{-1} for Q_{aq}/Q_{org} = 0.083) does not have a considerable influence on the oleic acid conversion for a given residence time (Figure 8b) and thus not on TON. Nevertheless, the interfacial area is affected significantly by a change in both Q_{aq}/Q_{org} (or β_{org}) and the wettability of the microreactor. The aqueous phase containing the enzyme was the continuous phase in the hydrophilic stainless steel microreactor and appeared as the discrete droplet in the hydrophobic PTFE microreactor. Thus, an increase in β_{org} resulted in relatively longer organic droplets in the former case, whereas in the latter case, shorter aqueous droplets were generated (Figure 10). Long droplets contribute to a considerable increase in the interfacial area that increased the reaction rate (Figure 10). Hence, the stainless steel microreactor is significantly more effective in terms of TON by operating at relatively high volumetric organic fractions than the PTFE microreactor and is thus more attractive for process intensification.

An interesting observation is that the kinetic model of Kraai et al.[27] does not fit well with the stainless steel microreactor data in terms of TON and especially the oleic acid conversion (Figures 9a,b). The actual slug flow profile in this microreactor is unknown, and the interfacial area therein was inferred from the glass capillary attached at its outlet (Figure 10). The interfacial area in the stainless steel microreactor might thus be different, which could affect the accuracy of the model estimation to some extent.

Moreover, in the stainless steel microreactor, there is an aqueous film surrounding the organic droplet. The film thickness (δ) can be estimated from[75]

$$\frac{\delta}{d_C} = \frac{0.66\mathrm{Ca}^{2/3}}{1 + 3.33\mathrm{Ca}^{2/3}} \tag{20}$$

where Ca is the capillary number defined by

$$\mathrm{Ca} = \frac{\mu_{aq} U_M}{\sigma} \tag{21}$$

DOI: 10.1021/acs.iecr.9b02693
Ind. Eng. Chem. Res. 2019, 58, 15432−15444

In this equation, μ_{aq} is the dynamic viscosity of the continuous phase (water; being 7.98×10^{-4} Pa s at 30 °C), and σ is the interfacial tension (50.30 mN m^{-1} at 30 °C for water−*n*-heptane system).[76]

Under typical reaction conditions relevant to Figure 9 (U_M = 12.7 cm min^{-1}), Ca is 3.37×10^{-5}, and the film thickness is 6.86×10^{-7} m in the stainless steel microreactor. Because of the thin aqueous film, the local specific interfacial area in the film (i.e., the total interfacial area of the film divided by the film volume) is high. Thus, it is likely that the enzyme amount in the liquid film was not high enough so that the interface in the film region may not be utilized sufficiently by the enzyme for the reaction (cf. eq 14). This means that the reaction rate is less enhanced by a further increase in the interfacial area (in the film region) as eq 18 implies. Thus, a more significant decrease in the oleic acid conversion compared with the model prediction at higher β_{org} values could be present given the more dominant contribution of the less active film region to the interfacial area (Figure 10). This could explain the model overestimation in the oleic acid conversion at much higher β_{org} values in this microreactor (Figure 9b). However, at much lower β_{org} values, the model should predict better since the aqueous film was much shorter, and the droplet caps have a more dominant contribution to the interfacial area (Figure 10). This is not in line with the observed model underestimation in Figure 9b under such circumstances; the reason of which is unknown and is an ongoing subject of our study.

In the PTFE microreactor, the enzyme was present in the aqueous droplet (Figure 10). Thus, it is expected that there was always enough enzyme available to exchange at the interface to catalyze the reaction, which was further facilitated by the enhanced mass transfer in the droplet due to inner circulation therein.[62,63]

3.4. Outlook. Although *n*-heptane was used in this work as a model organic solvent, for commercial applications, the reaction should be performed in more industrially attractive solvents. The use of other alkanes as solvents in an otherwise the same biphasic system was tested by Kraai et al.[27] High-molecular-weight alkanes (i.e., decane) resulted in a faster reaction rate due to a higher partition of 1-butanol toward the organic phase, increasing its concentration level therein. Conventional diesel (consisting of relatively long alkanes) could be a promising solvent, particularly for the production of (bio)diesel blends. Other low−molecular-weight alcohols (e.g., methanol and ethanol) can be used in the current microreactor system as well. However, in batch reactors, these were already shown to give lower reaction rates due to their lower solubility in the organic phase (*n*-heptane), which decreased the organic-phase alcohol concentration.[27] Relatively high-molecular-weight alcohols (e.g., 1-octanol), despite their higher partition coefficient, also decreased the reaction rate. It is likely that the long alkane tail of the alcohol decelerated binding with the enzyme by the increased steric hindrance as compared to smaller alcohols (e.g., 1-butanol).[27] Besides oleic acid esterification tested in this work, the current microreactor system could be used for the esterification of fatty acids, the transesterification of bio-based oils, and particularly oil sources having a relatively high free fatty acid content (e.g., waste cooking oils). However, it should be noted that the free lipase-catalyzed transesterification of triglycerides proceeds much slower than the fatty acid esterification in these biphasic systems, and as such considerably longer residence times are required.[30] Furthermore, the industrial-scale production of biodiesel in microreactors, despite their relatively easy scale-up, is challenging given the large production quantities required. As such, small-scale and localized (e.g., in rural areas) biodiesel production may be a more promising application for scaled-up microreactor processes.

The modeling and reactor engineering aspects presented in this work are not solely confined to the synthesis of biodiesel. Many other (free enzyme catalyzed) reactions in biphasic systems that take place on the liquid−liquid interface could benefit from the current findings.[77] These can be, for example, alternative lipase-catalyzed reactions for the production of esters or reactions using other enzymes (e.g., cellulase) that are activated on the liquid−liquid interface.

4. CONCLUSIONS

The enzymatic esterification of oleic acid with 1-butanol to butyl oleate was performed in a biphasic aqueous−organic system in capillary microreactors. The free *Rhizomucor miehei* lipase as the enzyme was dissolved in the aqueous phase, oleic acid in *n*-heptane and 1-butanol distributed over the two phases. The reaction temperature was 30 °C. No mass transfer limitations were observed in the PTFE microreactor operated under slug flow as indicated by no significant change in the oleic acid conversion while performing the reaction at the same residence time but different flow velocities. A close to 100% yield of butyl oleate could be achieved in the microreactor having an inner diameter of 0.8 mm within a residence time of 30 min. The increased interfacial area in smaller diameter microreactors significantly enhanced the reaction rate, given increased enzymatic activity by interfacial activation (i.e., more enzymes available to be bound to the interface). The reaction rate in the PTFE microreactor as a function of kinetic variables (i.e., enzyme and substrate concentration), the interfacial area, and the aqueous-to-organic volumetric flow ratio is well described by the literature kinetic model based on a Ping Pong Bi Bi mechanism with competitive inhibition of 1-butanol.[27] At relatively high volumetric organic fractions, the enzyme turnover number was enhanced significantly in the hydrophilic stainless steel microreactor as compared to the hydrophobic PTFE one, making the former microreactor promising for process intensification. However, due to the unknown flow profiles in the nontransparent stainless steel microreactor, its reaction performance in comparison with the kinetic model prediction needs to be further investigated. Although higher reaction rates can be obtained in optimized laboratory-scale batch reactors under intensive stirring than in microreactors used in this work, microreactors have the benefit of flow operation and relatively easy upscaling without a significant performance loss. Moreover, a precise control over parameters (among others interfacial area) in microreactors allows for more accurate kinetic investigations and the optimization of reaction conditions as demonstrated for the enzymatic biodiesel synthesis.

■ ASSOCIATED CONTENT

Supporting Information

The Supporting Information is available free of charge on the ACS Publications website at DOI: 10.1021/acs.iecr.9b02693.

Determination of the interfacial area and kinetic constant in a stirred batch reactor and determination of the oleic acid conversion from the kinetic model (PDF)

DOI: 10.1021/acs.iecr.9b02693
Ind. Eng. Chem. Res. 2019, 58, 15432−15444

AUTHOR INFORMATION

Corresponding Author

*E-mail: Yue.Jun@rug.nl.

ORCID

Jun Yue: 0000-0003-4043-0737

Notes

The authors declare no competing financial interest.

ACKNOWLEDGMENTS

This work was financially supported by the University of Groningen (startup package in the area of green chemistry and technology for J.Y.).

NOMENCLATURE

a	specific interfacial area, $m^2\ m^{-3}$
C	concentration, mol m^{-3}
Ca	capillary number
d	inner diameter, m
e	ellipticity of the oblate spheroid
E^*	superficial concentration of enzyme adsorbed on the interface, $g_{enz}\ m^{-2}$
k	kinetic constant, mol $L_{aq}\ g_{enz}^{-1}\ L_{org}^{-1}\ s^{-1}$
k''	kinetic constant based on interfacial area, mol m $g_{enz}^{-1}\ s^{-1}$
K_d^*	interfacial affinity constant, $g_{enz}\ L_{aq}^{-1}$
K_I	inhibition constant, mol L_{org}^{-1}
K_M	Michaelis–Menten constant, mol L_{org}^{-1}
L	length, m
m	partition coefficient
Q	volumetric flow rate, $m^3\ s^{-1}$
R	reaction rate, mol $L_{org}^{-1}\ s^{-1}$
R''	reaction rate based on interfacial area, mol m $L_{aq}^{-1}\ s^{-1}$
TON	enzyme turnover number, $mol_{FABE}\ g_{enz}^{-1}\ s^{-1}$
U	velocity, m s^{-1}
V	volume, m^3
X	conversion
Y	yield

GREEK LETTERS

β	phase volumetric fraction
δ	film thickness, m
μ	dynamic viscosity, Pa s
σ	surface tension, N m^{-1}
τ	residence time, s

SUBSCRIPTS

0	microreactor inlet
aq	aqueous phase
C	capillary microreactor
D	droplet
enz	enzyme
f	feed
M	two-phase mixture
org	organic phase
S	slug

ABBREVIATIONS

BuOH	1-butanol
FABE	fatty acid butyl ester (butyl oleate)
FA	fatty acid (oleic acid)
RML	*Rhizomucor miehei* lipase

REFERENCES

(1) Ma, F.; Hanna, M. A. Biodiesel Production: A review. *Bioresour. Technol.* **1999**, *70*, 1.

(2) Meher, L.; Vidyasagar, D.; Naik, S. Technical Aspects of Biodiesel Production by Transesterification—a Review. *Renewable Sustainable Energy Rev.* **2006**, *10*, 248.

(3) Demirbas, A. Progress and Recent Trends in Biodiesel Fuels. *Energy Convers. Manage.* **2009**, *50*, 14.

(4) Atadashi, I. M.; Aroua, M. K.; Aziz, A. A. High Quality Biodiesel and Its Diesel Engine Application: A Review. *Renewable Sustainable Energy Rev.* **2010**, *14*, 1999.

(5) Suehara, K.; Kawamoto, Y.; Fujii, E.; Kohda, J.; Nakano, Y.; Yano, T. Biological Treatment of Wastewater Discharged from Biodiesel Fuel Production Plant with Alkali-Catalyzed Transesterification. *J. Biosci. Bioeng.* **2005**, *100*, 437.

(6) Nielsen, P. M.; Brask, J.; Fjerbaek, L. Enzymatic Biodiesel Production: Technical and Economical Considerations. *Eur. J. Lipid Sci. Technol.* **2008**, *110*, 692.

(7) Du, W.; Li, W.; Sun, T.; Chen, X.; Liu, D. Perspectives for Biotechnological Production of Biodiesel and Impacts. *Appl. Microbiol. Biotechnol.* **2008**, *79*, 331.

(8) Fjerbaek, L.; Christensen, K. V.; Norddahl, B. A Review of the Current State of Biodiesel Production Using Enzymatic Transesterification. *Biotechnol. Bioeng.* **2009**, *102*, 1298.

(9) Robles-Medina, A.; González-Moreno, P. A.; Esteban-Cerdán, L.; Molina-Grima, E. Biocatalysis: Towards Ever Greener Biodiesel Production. *Biotechnol. Adv.* **2009**, *27*, 398.

(10) Gog, A.; Roman, M.; Toşa, M.; Paizs, C.; Irimie, F. D. Biodiesel Production Using Enzymatic Transesterification - Current State and Perspectives. *Renewable Energy* **2012**, *39*, 10.

(11) Dossat, V.; Combes, D.; Marty, A. Lipase-Catalysed Transesterification of High Oleic Sunflower Oil. *Enzyme Microb. Technol.* **2002**, *30*, 90.

(12) Ghaly, A. E.; Dave, D.; Brooks, M. S.; Budge, S. Production of Biodiesel by Enzymatic Transesterification: Review. *Am. J. Biochem. Biotechnol.* **2010**, *6*, 54.

(13) Zhang, Y.; Dubé, M. A.; McLean, D. D.; Kates, M. Biodiesel Production from Waste Cooking Oil: 1. Process Design and Technological Assessment. *Bioresour. Technol.* **2003**, *89*, 1.

(14) Kulkarni, M. G.; Dalai, A. K. Waste Cooking Oil - An Economical Source for Biodiesel: A Review. *Ind. Eng. Chem. Res.* **2006**, *45*, 2901.

(15) Lam, M. K.; Lee, K. T.; Mohamed, A. R. Homogeneous, Heterogeneous and Enzymatic Catalysis for Transesterification of High Free Fatty Acid Oil (Waste Cooking Oil) to Biodiesel: A Review. *Biotechnol. Adv.* **2010**, *28*, 500.

(16) Bajaj, A.; Lohan, P.; Jha, P. N.; Mehrotra, R. Biodiesel Production through Lipase Catalyzed Transesterification: An Overview. *J. Mol. Catal. B: Enzym.* **2010**, *62*, 9.

(17) Tan, T.; Lu, J.; Nie, K.; Deng, L.; Wang, F. Biodiesel Production with Immobilized Lipase: A Review. *Biotechnol. Adv.* **2010**, *28*, 628.

(18) Chesterfield, D. M.; Rogers, P. L.; Al-Zaini, E. O.; Adesina, A. A. Production of Biodiesel via Ethanolysis of Waste Cooking Oil Using Immobilised Lipase. *Chem. Eng. J.* **2012**, *207-208*, 701.

(19) Sheldon, R. A. Enzyme Immobilization: The Quest for Optimum Performance. *Adv. Synth. Catal.* **2007**, *349*, 1289.

(20) Brzozowski, A. M.; Derewenda, U.; Derewenda, Z. S.; Dodson, G. G.; Lawson, D. M.; Turkenburg, J. P.; Bjorkling, F.; Huge-Jensen, B.; Patkar, S. A.; Thim, L. A Model for Interfacial Activation in Lipases from the Structure of a Fungal Lipase-Inhibitor Complex. *Nature* **1991**, *351*, 491.

(21) Verger, R. "Interfacial Activation" of Lipases: Facts and Artifacts. *Trends Biotechnol.* **1997**, *15*, 32.

(22) Rehm, S.; Trodler, P.; Pleiss, J. Solvent-Induced Lid Opening in Lipases: A Molecular Dynamics Study. *Protein Sci.* **2010**, *19*, 2122.

(23) Tsai, S.-W.; Chang, C.-S. Kinetics of Lipase-catalyzed Hydrolysis of Lipids in Biphasic Organic—Aqueous Systems. *J. Chem. Technol. Biotechnol.* **1993**, *57*, 147.

DOI: 10.1021/acs.iecr.9b02693
Ind. Eng. Chem. Res. 2019, 58, 15432−15444

(24) Rooney, D.; Weatherley, L. R. The Effect of Reaction Conditions upon Lipase Catalysed Hydrolysis of High Oleate Sunflower Oil in a Stirred Liquid-Liquid Reactor. *Process Biochem.* **2001**, *36*, 947.
(25) Čech, J.; Schrott, W.; Slouka, Z.; Přibyl, M.; Brož, M.; Kuncová, G.; Šnita, D. Enzyme Hydrolysis of Soybean Oil in a Slug Flow Microsystem. *Biochem. Eng. J.* **2012**, *67*, 194.
(26) Oliveira, A. C.; Rosa, M. F.; Aires-Barros, M. R.; Cabral, J. M. S. Enzymatic Esterification of Ethanol and Oleic Acid - A Kinetic Study. *J. Mol. Catal. B: Enzym.* **2001**, *11*, 999.
(27) Kraai, G. N.; Winkelman, J. G. M.; de Vries, J. G.; Heeres, H. J. Kinetic Studies on the Rhizomucor Miehei Lipase Catalyzed Esterification Reaction of Oleic Acid with 1-Butanol in a Biphasic System. *Biochem. Eng. J.* **2008**, *41*, 87.
(28) Al-Zuhair, S.; Jayaraman, K. V.; Krishnan, S.; Chan, W.-H. The Effect of Fatty Acid Concentration and Water Content on the Production of Biodiesel by Lipase. *Biochem. Eng. J.* **2006**, *30*, 212.
(29) Oliveira, A. C.; Rosa, M. F. Enzymatic Transesterification of Sunflower Oil in an Aqueous-Oil Biphasic System. *J. Am. Oil Chem. Soc.* **2006**, *83*, 21.
(30) Ilmi, M.; Hommes, A.; Winkelman, J. G. M.; Hidayat, C.; Heeres, H. J. Kinetic Studies on the Transesterification of Sunflower Oil with 1-Butanol Catalyzed by Rhizomucor Miehei Lipase in a Biphasic Aqueous-Organic System. *Biochem. Eng. J.* **2016**, *114*, 110.
(31) Qiu, Z.; Zhao, L.; Weatherley, L. Process Intensification Technologies in Continuous Biodiesel Production. *Chem. Eng. Process. Process Intensif.* **2010**, *49*, 323.
(32) Maddikeri, G. L.; Pandit, A. B.; Gogate, P. R. Intensification Approaches for Biodiesel Synthesis from Waste Cooking Oil: A Review. *Ind. Eng. Chem. Res.* **2012**, *51*, 14610.
(33) Kraai, G. N.; Van Zwol, F.; Schuur, B.; Heeres, H. J.; De Vries, J. G. Two-Phase (Bio)Catalytic Reactions in a Table-Top Centrifugal Contact Separator. *Angew. Chem., Int. Ed.* **2008**, *47*, 3905.
(34) Ilmi, M.; Abduh, M. Y.; Hommes, A.; Winkelman, J. G. M.; Hidayat, C.; Heeres, H. J. Process Intensification of Enzymatic Fatty Acid Butyl Ester Synthesis Using a Continuous Centrifugal Contactor Separator. *Ind. Eng. Chem. Res.* **2018**, *57*, 470.
(35) Ilmi, M.; Kloekhorst, A.; Winkelman, J. G. M.; Euverink, G. J. W.; Hidayat, C.; Heeres, H. J. Process Intensification of Catalytic Liquid-Liquid Solid Processes: Continuous Biodiesel Production Using an Immobilized Lipase in a Centrifugal Contactor Separator. *Chem. Eng. J.* **2017**, *321*, 76.
(36) Oliveira, A. C.; Rosa, M. F.; Aires-Barros, M. R.; Cabral, J. M. S. Enzymatic Esterification of Ethanol by an Immobilised Rhizomucor Miehei Lipase in a Perforated Rotating Disc Bioreactor. *Enzyme Microb. Technol.* **2000**, *26*, 446.
(37) Chesterfield, D. M.; Trung, T. C.; Lucien, F. P.; Rogers, P. L.; Adesina, A. A. Basket Impeller Extractive Reactor Column for Biodiesel Production: An Experimental Study. *Ind. Eng. Chem. Res.* **2013**, *52*, 15298.
(38) Nioi, C.; Riboul, D.; Destrac, P.; Marty, A.; Marchal, L.; Condoret, J. S. The Centrifugal Partition Reactor, a Novel Intensified Continuous Reactor for Liquid-Liquid Enzymatic Reactions. *Biochem. Eng. J.* **2015**, *103*, 227.
(39) Nioi, C.; Destrac, P.; Condoret, J. S. Lipase Esterification in the Centrifugal Partition Reactor: Modelling and Determination of the Specific Interfacial Area. *Biochem. Eng. J.* **2019**, *143*, 179.
(40) Xie, T.; Zhang, L.; Xu, N. Biodiesel Synthesis in Microreactors. *Green Process. Synth.* **2012**, *1*, 61.
(41) Madhawan, A.; Arora, A.; Das, J.; Kuila, A.; Sharma, V. Microreactor Technology for Biodiesel Production: A Review. *Biomass Convers. Biorefin.* **2018**, *8*, 485.
(42) Tiwari, A.; Rajesh, V. M.; Yadav, S. Biodiesel Production in Micro-Reactors: A Review. *Energy Sustainable Dev.* **2018**, *43*, 143.
(43) Dençić, I.; De Vaan, S.; Noël, T.; Meuldijk, J.; De Croon, M.; Hessel, V. Lipase-Based Biocatalytic Flow Process in a Packed-Bed Microreactor. *Ind. Eng. Chem. Res.* **2013**, *52*, 10951.
(44) Bi, Y.; Zhou, H.; Jia, H.; Wei, P. A Flow-through Enzymatic Microreactor Immobilizing Lipase Based on Layer-by-Layer Method for Biosynthetic Process: Catalyzing the Transesterification of Soybean Oil for Fatty Acid Methyl Ester Production. *Process Biochem.* **2017**, *54*, 73.
(45) He, P.; Greenway, G.; Haswell, S. J. Development of a Monolith Based Immobilized Lipase Micro-Reactor for Biocatalytic Reactions in a Biphasic Mobile System. *Process Biochem.* **2010**, *45*, 593.
(46) Machsun, A. L.; Gozan, M.; Nasikin, M.; Setyahadi, S.; Yoo, Y. J. Membrane Microreactor in Biocatalytic Transesterification of Triolein for Biodiesel Production. *Biotechnol. Bioprocess Eng.* **2010**, *15*, 911.
(47) Budžaki, S.; Miljić, G.; Tišma, M.; Sundaram, S.; Hessel, V. Is There a Future for Enzymatic Biodiesel Industrial Production in Microreactors? *Appl. Energy* **2017**, *201*, 124.
(48) Habibi, A.; Fahim, S.; Shirvani, N.; Rahimi, M. Enzymatic Methanolysis Reaction of Canola Oil Using Capillary Channel Reactor: Determination of the Kinetic Constants-Involved. *J. Mol. Catal. B: Enzym.* **2016**, *132*, 47.
(49) Elgue, S.; Conté, A.; Marty, A.; Condoret, J.-S. Continuous Lipase Esterification Using Process Intensification Technologies. *J. Chem. Technol. Biotechnol.* **2014**, *89*, 1590.
(50) Geyer, K.; Codée, J. D. C.; Seeberger, P. H. Microreactors as Tools for Synthetic Chemists—The Chemists' Round-Bottomed Flask of the 21st Century? *Chem. − Eur. J.* **2006**, *12*, 8434.
(51) Mills, P. L.; Quiram, D. J.; Ryley, J. F. Microreactor Technology and Process Miniaturization for Catalytic Reactions-A Perspective on Recent Developments and Emerging Technologies. *Chem. Eng. Sci.* **2007**, *62*, 6992.
(52) Yue, J. Multiphase Flow Processing in Microreactors Combined with Heterogeneous Catalysis for Efficient and Sustainable Chemical Synthesis. *Catal. Today* **2018**, *308*, 3.
(53) Trachsel, F.; Günther, A.; Khan, S.; Jensen, K. F. Measurement of Residence Time Distribution in Microfluidic Systems. *Chem. Eng. Sci.* **2005**, *60*, 5729.
(54) Woitalka, A.; Kuhn, S.; Jensen, K. F. Scalability of Mass Transfer in Liquid-Liquid Flow. *Chem. Eng. Sci.* **2014**, *116*, 1.
(55) Yue, J.; Boichot, R.; Luo, L.; Gonthier, Y.; Chen, G.; Yuan, Q. Flow Distribution and Mass Transfer in a Parallel Microchannel Contactor Integrated with Constructal Distributors. *AIChE J.* **2010**, *56*, 298.
(56) Ghaini, A.; Kashid, M. N.; Agar, D. W. Effective Interfacial Area for Mass Transfer in the Liquid-Liquid Slug Flow Capillary Microreactors. *Chem. Eng. Process. Process Intensif.* **2010**, *49*, 358.
(57) Susanti; Winkelman, J. G. M.; Schuur, B.; Heeres, H. J.; Yue, J. Lactic Acid Extraction and Mass Transfer Characteristics in Slug Flow Capillary Microreactors. *Ind. Eng. Chem. Res.* **2016**, *55*, 4691.
(58) García, V.; Päkkilä, J.; Ojamo, H.; Muurinen, E.; Keiski, R. L. Challenges in Biobutanol Production: How to Improve the Efficiency? *Renewable Sustainable Energy Rev.* **2011**, *15*, 964.
(59) Rodrigues, R. C.; Fernandez-Lafuente, R. Lipase from Rhizomucor Miehei as a Biocatalyst in Fats and Oils Modification. *J. Mol. Catal. B: Enzym.* **2010**, *66*, 15.
(60) Ulberth, F.; Gabernig, R. G.; Schrammel, F. Flame-Ionization Detector Response to Methyl, Ethyl, Propyl, and Butyl Esters of Fatty Acids. *J. Am. Oil Chem. Soc.* **1999**, *76*, 263.
(61) van Baten, J. M.; Krishna, R. CFD Simulations of Mass Transfer from Taylor Bubbles Rising in Circular Capillaries. *Chem. Eng. Sci.* **2004**, *59*, 2535.
(62) Kashid, M. N.; Harshe, Y. M.; Agar, D. W. Liquid-Liquid Slug Flow in a Capillary: An Alternative to Suspended Drop or Film Contactors. *Ind. Eng. Chem. Res.* **2007**, *46*, 8420.
(63) Dessimoz, A. L.; Cavin, L.; Renken, A.; Kiwi-Minsker, L. Liquid-Liquid Two-Phase Flow Patterns and Mass Transfer Characteristics in Rectangular Glass Microreactors. *Chem. Eng. Sci.* **2008**, *63*, 4035.
(64) van Steijn, V.; Kreutzer, M. T.; Kleijn, C. R. μ-PIV Study of the Formation of Segmented Flow in Microfluidic T-Junctions. *Chem. Eng. Sci.* **2007**, *62*, 7505.

DOI: 10.1021/acs.iecr.9b02693
Ind. Eng. Chem. Res. 2019, 58, 15432−15444

(65) Abate, A. R.; Poitzsch, A.; Hwang, Y.; Lee, J.; Czerwinska, J.; Weitz, D. A. Impact of Inlet Channel Geometry on Microfluidic Drop Formation. *Phys. Rev. E* **2009**, *80*, 026310.
(66) Hari Krishna, S.; Karanth, N. G. Lipases and Lipase-Catalyzed Esterification Reactions in Nonaqueous Media. *Catal. Rev.* **2002**, *44*, 499.
(67) Cajal, Y.; Svendsen, A.; De Bolós, J.; Patkar, S. A.; Alsina, M. A. Effect of the Lipid Interface on the Catalytic Activity and spectroscopic Properties of a Fungal Lipase. *Biochimie* **2000**, *82*, 1053.
(68) Straathof, A. J. J. Enzymatic Catalysis via Liquid-Liquid Interfaces. *Biotechnol. Bioeng.* **2003**, *83*, 371.
(69) Afshar Ghotli, R.; Raman, A. A. A.; Ibrahim, S.; Baroutian, S. Liquid-Liquid Mixing in Stirred Vessels: A Review. *Chem. Eng. Commun.* **2013**, *200*, 595.
(70) Quadros, P. A.; Baptista, C. M. S. G Effective Interfacial Area in Agitated Liquid-Liquid Continuous Reactors. *Chem. Eng. Sci.* **2003**, *58*, 3935.
(71) Al-Zuhair, S.; Ling, F. W.; Jun, L. S. Proposed Kinetic Mechanism of the Production of Biodiesel from Palm Oil Using Lipase. *Process Biochem.* **2007**, *42*, 951.
(72) Winkelman, J. G. M.; Kraai, G. N.; Heeres, H. J. Binary, Ternary and Quaternary Liquid-Liquid Equilibria in 1-Butanol, Oleic Acid, Water and n-Heptane Mixtures. *Fluid Phase Equilib.* **2009**, *284*, 71.
(73) Saktaweewong, S.; Phinyocheep, P.; Ulmer, C.; Marie, E.; Durand, A.; Inprakhon, P. Lipase Activity in Biphasic Media: Why Interfacial Area Is a Significant Parameter? *J. Mol. Catal. B: Enzym.* **2011**, *70*, 8.
(74) Kreutzer, M. T.; Kapteijn, F.; Moulijn, J. A.; Heiszwolf, J. J. Multiphase Monolith Reactors: Chemical Reaction Engineering of Segmented Flow in Microchannels. *Chem. Eng. Sci.* **2005**, *60*, 5895.
(75) Aussillous, P.; Quéré, D. Quick Deposition of a Fluid on the Wall of a Tube. *Phys. Fluids* **2000**, *12*, 2367.
(76) Zeppieri, S.; Rodríguez, J.; López De Ramos, A. L. Interfacial Tension of Alkane + Water Systems. *J. Chem. Eng. Data* **2001**, *46*, 1086.
(77) Reis, P.; Holmberg, K.; Watzke, H.; Leser, M. E.; Miller, R. Lipases at Interfaces: A Review. *Adv. Colloid Interface Sci.* **2009**, *147-148*, 237.

DOI: 10.1021/acs.iecr.9b02693
Ind. Eng. Chem. Res. 2019, 58, 15432−15444